
ELECTROMOTION

**Volume 10, Number 3
July – September 2003**

Special Issue :

**Proceedings of the 5th International
Symposium on Advanced Electromechanical
Motion Systems
ELECTROMOTION 2003, (Vol. 1)
Marrakesh, Morocco, November 26-28, 2003**



utbm
UNIVERSITÉ DE TECHNOLOGIE
DE BELFORT-MONTBÉLIARD



Université Cadi Ayyad

**AN INTERNATIONAL JOURNAL DEVOTED
TO RESEARCH, DEVELOPMENT, DESIGN AND
APPLICATION OF ELECTROMECHANICAL ENERGY
CONVERTERS, ACTUATORS AND TRANSDUCERS**

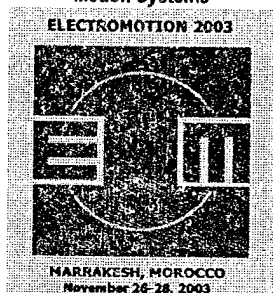
Modelling and performance analysis of induction machines

- Jumei Cai, G. Henneberger* Development of a bearingless wound-rotor induction machine 153
- W.R. Canders, H. Mosebach* Simple two-dimensional analytical model for induction machines with a very large air-gap 159
- L. Chen, L.J. Hou* Study on steady-state performance of a 15-phase induction machine under asymmetrical connections 165
- C. Constantinescu, D. Mihai* A neuro-fuzzy model for induction motor drives 171
- N. Erdogan, R. Grisel* Dynamic modelling of three-phase induction machines with skin effect and saturation effects for transient studies 175
- R. Wamkeue, D. Aguglia, I. Kamwa* Saturated electromechanical Simulink block-diagram model of induction machine 180
- A. Campeanu, I. Vlad, A. Ionescu, S. Enache* Establishment of optimal constructive dimensions of electrical machines 187
- O.Gh. Draganescu* Analytical study and experimental methods for determination of the reluctance additional iron losses of induction machine 193
- L. Livadaru, A. Simion* Performance analysis of a two-phase induction motor with salient stator poles and radial assembled laminations 199
- Vasilija Sarac, Lidija Petkovska* A novel approach to performance characteristics evaluation of a shaded-pole induction motor 205

Design and control of permanent-magnet synchronous motors

- E. Akpinar, O. Gergoz, C. Cengiz* Design and control of exterior-rotor brushless DC motor for fan-type load 211
- M. Bertoluzzo, G. Buja, E. Stampacchia, S. Zago* Brushless AC servo systems: internal torque disturbances and their compensation 217
- Chiara Boccaletti, C. Bruzzese, E. Santini, P. Sordi* Accurate design of axial-flux permanent-magnet synchronous machines by means of three-dimensional finite element analysis 223

5th International Symposium on
Advanced Electromechanical
Motion Systems



A NOVEL APPROACH TO PERFORMANCE CHARACTERISTICS EVALUATION OF A SHADED-POLE INDUCTION MOTOR

Vasilija Sarac* and Lidija Petkovska**

* 'St. Clement Ohridski' University
Faculty of Technical Sciences
P.O. Box 99, 7000 Bitola, Macedonia
vasilija.sarac@siemens.com.mk

** 'Ss. Cyril and Methodius' University
Faculty of Technical Sciences
P.O. Box 574, 1000 Skopje, Macedonia
lidijap@etf.edu.mk

Abstract- In the paper a novel approach to the modeling and simulation of shaded-pole induction motor, aiming towards the evaluation of its performance characteristics at different load conditions is presented. For this purpose, different methods for analysis, as analytic Circuit Theory Method (CTM), numerical Finite Element Method (FEM) and simulation Matlab/Simulink Method (MSM) are applied. The proposed approach is valid both for steady state and transient regimes. A complex modeling of the shaded-pole induction motor, in order to derive the most suitable models for application of the proposed methods, is carried out. On the basis of the analysis of the performance characteristics, each of the methods is going to be evaluated. The results of analytical and numerical calculations, as well as simulations, are compared with experimentally obtained ones, and/or with the known values given by the producer; they show a reasonable agreement, proving the proposed approach as accurate.

I. INTRODUCTION

Single-phase shaded-pole motors have found wide fractional horsepower applications in many household devices due to their simple construction, low costs, as well as their capability for sustaining overloading in locked rotor position since the value of short circuit current is very close to the value of rated current. In spite of that, their analysis is always complicated due to their particular arrangements of windings, elliptically rotating air gap magnetic field, and a significant level of the space harmonics. Over the past decades many researches [1-4] have paid a considerable attention to the solution of the problems related to the most exact prediction of performance characteristics of shaded-pole induction motors. Some authors use the simulation techniques and the analytical method based on the revolving field theory and the decomposition of the air-gap field in two components, forward and backward. The others prefer to use numerical methods, based on the application of Finite Element techniques. Simulation of transient performance and dynamic characteristics by using the Simulation methodology is widely used in recent years. However, it can be easily concluded, that a commonly accepted approach does not exist so far.

II. SHADED-POLE INDUCTION MOTOR

In this paper, the authors present a novel approach to the evaluation of performance characteristics of a shaded-pole motor, by using analytical, numerical and simulation methods. The test results, as well as some of the known data from the producer, are used for evaluation of each of

the proposed methods. After a detailed analysis of the computed characteristics is carried out, the comparison of the methods will be done.

As an object of investigation in the paper is considered a single-phase shaded-pole induction motor, type AKO-16, produced by "Mikron" with rated data: $U_n=220$ V; $f_n=50$ Hz, $I_{ln}=0.125$ A; $P_{ln}=18$ W; $n_n=2520$ rpm; $2p=2$. The number of turns of main stator winding is 1744 per pole. The shading coil has one winding per pole, while the shading portion of the stator pole cross section is 25 %, i.e. $\gamma=0.238$ rad. A view of the geometrical cross section of the motor is presented in Fig. 1.

III. METHODOLOGY

The proposed approach for complex analysis of the shaded-pole induction motor comprehends the application of different methods as: Circuit Theory Method (CTM), Finite Element Method (FEM) and Matlab/Simulink (MSM). By the means of each method, the steady state and transient performance characteristics of the motor are determined.

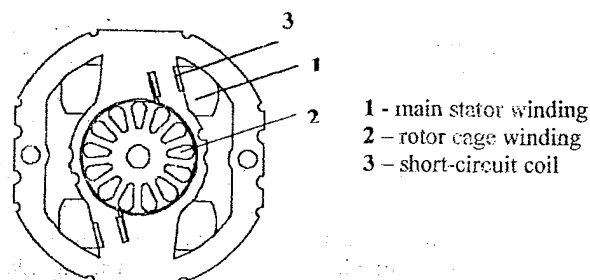


Fig. 1. Geometrical cross-section of the motor

A development of different mathematical models, suitable for application of different methods, is carried out. The shaded-pole induction motor is analysed at no-load, locked-rotor and different running and loading conditions.

A. Circuit Theory Method -CTM

The Circuit Theory Method, as an analytical method, is especially convenient for the steady state performance analysis of shaded-pole motor [1]. Instead of the real motor consisted of electromagnetic linked circuits, equivalent electrical circuits, developed on the basis of revolving field theory decomposition are considered. In the single-phase shaded-pole motor exist two separate windings which are space shifted by an angle $\alpha \neq 0^\circ$ and consequently currents which flows through both stator windings (main 1 and short circuit coil 3) are time shifted by an angle $\beta \neq 0^\circ$. On that way, the vector of magnetic flux describes an ellipse. The electromagnetic field inside the motor, is analyzed by the method of symmetrical components. Hence, the stator currents are calculated from:

$$I_1 = -j \left(\frac{I_1^- e^{j\alpha}}{\sin \alpha} - \frac{I_1^+ e^{-j\alpha}}{\sin \alpha} \right) \quad (1)$$

$$I_3 = j \left(\frac{I_1^-}{\sin \alpha} - \frac{I_1^+}{\sin \alpha} \right) \quad (2)$$

Symmetrical components of stator currents can be found from following equations:

$$I_1^- = \frac{I_1^+ (jZ_{1b} - e^{-j\alpha} Z^+ \sin \alpha - je^{-j\alpha} Z_{ab} + jZ_{ab})}{jZ_{1b} + e^{j\alpha} Z^- \sin \alpha - je^{j\alpha} Z_{ab} + jZ_{ab}} \quad (3)$$

$$I_1^+ = \frac{V_1 \sin \alpha (jZ_{1b} + e^{j\alpha} Z^- \sin \alpha - je^{j\alpha} Z_{ab} + jZ_{ab})}{(A \cdot B) + (C \cdot D)} \quad (4)$$

where:

$$A = jZ_{1b} - e^{-j\alpha} Z^+ \sin \alpha - je^{-j\alpha} Z_{ab} + jZ_{ab} \quad (5)$$

$$B = je^{j\alpha} Z_{1a} - Z^- \sin \alpha + je^{j\alpha} Z_{ab} - jZ_{ab} \quad (6)$$

$$C = jZ_{ab} - Z^+ \sin \alpha - je^{-j\alpha} Z_{ab} - je^{-j\alpha} Z_{1a} \quad (7)$$

$$D = jZ_{1b} + e^{j\alpha} Z^- \sin \alpha - je^{j\alpha} Z_{ab} + jZ_{ab} \quad (8)$$

For impedances the following expressions are valid:

$$Z^+ = \frac{Z_0 Z_2^+}{Z_2^+ + Z_0} \quad Z^- = \frac{Z_0 Z_2^-}{Z_2^- + Z_0} \quad Z_2^+ = \frac{R_2'}{s} + jX_2' \quad (9)$$

$$Z_2^- = \frac{R_2'}{2-s} + jX_2' \quad Z_0 = R_0 + jX_0 \quad (10)$$

Z_{1a} and Z_{1b} are consequently impedances of main stator winding and short circuit co; Z_{ab} is mutual impedance between main stator winding and short circuit coil; Z_0 is the magnetizing impedance; while, R_2' and X_2' are the

rotor parameters. The angle α is a space angle between axes of symmetry of main stator winding and short circuit coil, and for the analyzed motor its value is 43.4° . Symmetrical components of rotor currents can be found from the expressions:

$$I_2^+ = I_1^+ \frac{Z_0}{Z_0 + Z_2^+} \quad I_2^- = I_1^- \frac{Z_0}{Z_0 + Z_2^-} \quad (11)$$

Electromagnetic torque can be calculated from symmetrical components of rotor currents, as:

$$M_{em}^+ = \frac{9,55}{n_s} \frac{2|I_2^+|^2 R_2'}{s} \quad M_{em}^- = \frac{9,55}{n_s} \frac{2|I_2^-|^2 R_2'}{2-s} \quad (12)$$

In Table 1, the results from CTM calculations at rated load condition, are compared with experimental data; they show very good agreement. Performance characteristics obtained from CTM are presented in Fig. 2 and Fig. 3.

Table 1
Comparison of results from CTM and experiment

CTM	Experiment
$I_1 = 0.125$ A	$I_1 = 0.1259$ A
$P_1 = 18.114$ W	$P_1 = 18$ W
$\cos \phi = 0.65389$	$\cos \phi = 0.654$
$n = 2520$ rpm	$n = 2120$ rpm

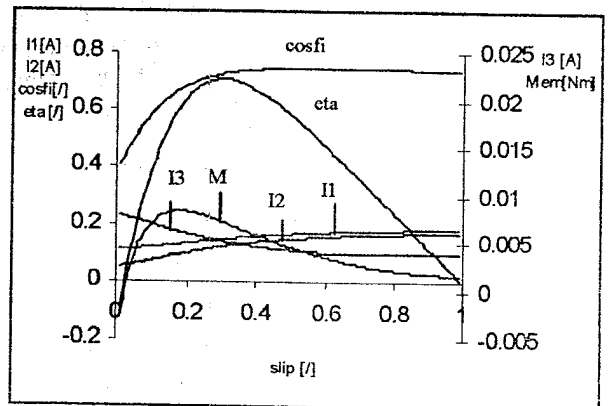


Fig. 2. Performance characteristics from CTM

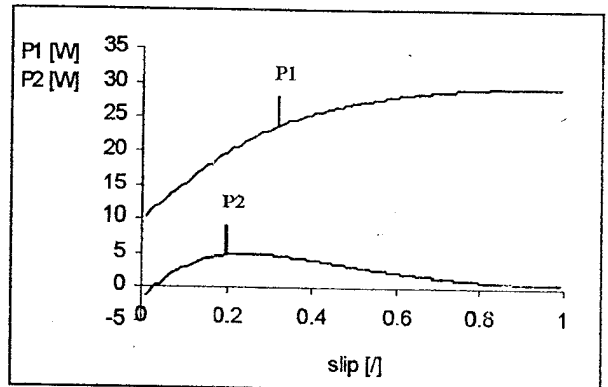


Fig. 3. Electric power characteristics from CTM

B. Finite Element – Method

The Finite Element Method is widely used in the numerical analysis of electrical machines. In the FEM analysis of the shaded-pole motor, the most interesting are time domain harmonic solutions, under different operating conditions. Taking into consideration the compound configuration of the shaded-pole induction motor, both in electrical and magnetic sense, a model suitable for implementation of FEM is derived [3]. For the purpose of this analysis, the mesh is spread over the whole cross-section of the motor, and is consisted of 10,250 nodes and 20,063 elements.

The main stator winding is energized with currents corresponding to different load conditions i.e. slips, while currents both in stator shading coil and rotor bars are induced. Since the non-linear time harmonic analysis is performed, stator quantities are oscillating with one fix frequency i.e. $f=50$ Hz, while the rotor quantities oscillate at slip frequency, quite different from the stator frequency. The problem is solved by adjusting the rotor bars conductivity σ corresponding to the slip. Hence the non-linear time harmonic analysis by using FEM, is performed at fixed stator winding supply frequency $f=50$ Hz, while the rotor slip is changing with the load.

In Figures 4, 5 and 6 are presented flux distributions in the middle of the cross-section of shaded-pole motor at following operating modes: no load at current $I_s=0.111$ A and slip $s=0$; locked rotor (start-up) at current $I_s=0.135$ A and slip $s=1.0$; rated load at current $I_s=0.125$ A and slip $s=0.16$. The number of flux lines in the previously mentioned figures is selected to be proportional to the field strength, and the difference of the field intensity is seen.

The non-linear FEM harmonic analysis offers possibility to get "inside" the motor and to find its "weak" parts i.e. areas with high saturation and, if requested, to improve its design features.

One of the most interesting parameters of the motors is always electromagnetic torque. Hence, the authors paid a special attention to its computation and verification of obtained results. Electromagnetic torque is calculated numerically by the electromagnetic force, via Maxwell's Stress Tensor. The stress tensor can be evaluated over a contour away from the surface of the object, where the field solution is much more accurate. The best results are obtained by integrating along the contour a few elements away from any boundary or interface.

The torque is easily derived from the tangential components of the force, by using the following expression:

$$M_{em} = \left[\frac{r}{\mu_0} \oint (E_n \cdot B_t) dc \right] l_s \quad (13)$$

where: B_n and B_t are normal and tangential components of the magnetic flux density; c is integration contour; r is a distance of the integrating path from the center of rotation; l_s is axial rotor length.

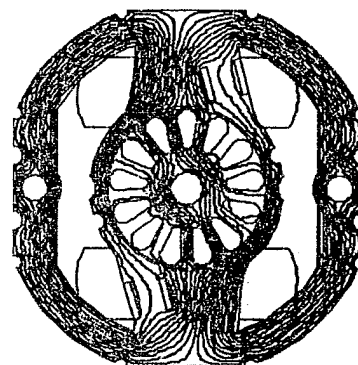


Fig. 4. Magnetic flux distribution at no-load

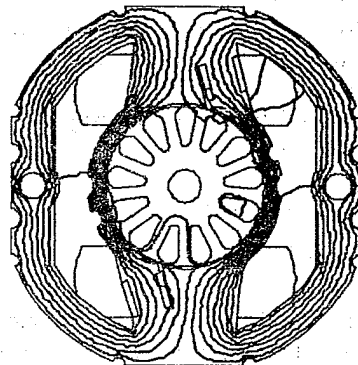


Fig. 5. Magnetic flux distribution at locked rotor

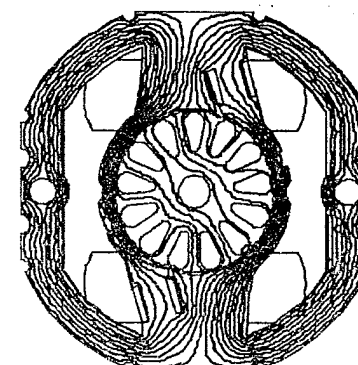


Fig. 6. Magnetic flux distribution at rated load

C. Matlab/Simulink Method –MSM

Matlab/Simulink is widely known powerful simulation tool which enables to view and analyze motor transient performance characteristics [4]. When simulation methods are used, main emphasis has to be put on development of proper mathematical method, which will represent the physical phenomena as close as possible. The derived model of shaded-pole motor, suitable for implementation in Matlab/Simulink bases on d,q transformation known from reference frame theory of single-phase induction machines [5-6].

Two phase power supply is modelled using following equations:

$$\mathbf{f}_{qs} = \mathbf{K}_{2s} \mathbf{f}_{abs} \quad (14)$$

$$(\mathbf{f}_{qds})^T = [f_{as} \quad f_{ds}] \quad (15)$$

$$(\mathbf{f}_{abs})^T = [f_{as} \quad f_{bs}] \quad (16)$$

$$\mathbf{K}_{2s} = \begin{bmatrix} \cos \theta & \sin \theta \\ \sin \theta & -\cos \theta \end{bmatrix} \quad (17)$$

where $\theta = \int \omega dt$,

f represents stator and/or rotor variables.

For single-phase motor transformation of stator and rotor variables is made in d,q system which is stationary, meaning $\omega = 0$.

Using (14) for modeling of two phase power supply, the following equations are valid:

$$U_{qs} = U_{as} \cos \theta + U_{bs} \sin \theta \quad (18)$$

$$U_{ds} = U_{as} \sin \theta - U_{bs} \cos \theta \quad (19)$$

Influence of the shading coil ring is taken into account by introducing the phase shift between voltage sources U_{as} and U_{bs} , which for analysed motor is determined as 43.4° . For simulation purposes voltage equation of stator and rotor circuits are rearranged in the following form:

$$\begin{aligned} i_{qs} &= \frac{1}{L_{lqs} + L_{mq}} \int U_{qs} - \frac{r_{qs}}{L_{lqs} + L_{mq}} \int i_{qs} - \frac{L_{mq}}{L_{lqs} + L_{mq}} i_{qr}^s \\ i_{ds} &= \frac{1}{L_{lds} + L_{mq}} \int U_{ds} - \frac{r_{ds}}{L_{lds} + L_{mq}} \int i_{ds} - \frac{L_{mq}}{L_{lds} + L_{mq}} i_{dr}^s \\ i_{qr}^s &= \omega_r \int i_{dr}^s + \frac{\omega_r L_{mq}}{L_{lr} + L_{mq}} \int i_{ds} - \frac{r_r}{L_{lr} + L_{mq}} \int i_{qr}^s - \frac{L_{mq}}{L_{lr} + L_{mq}} i_{qs} \\ i_{dr}^s &= -\omega_r \int i_{qr}^s - \frac{\omega_r L_{mq}}{L_{lr} + L_{mq}} \int i_{qs} - \frac{r_r}{L_{lr} + L_{mq}} \int i_{dr}^s - \frac{L_{mq}}{L_{lr} + L_{mq}} i_{ds} \end{aligned} \quad (20)$$

r_{qs} , r'_{ds} and r_r are resistances of main winding, short circuit coil and rotor, winding respectively. L_{lqs} , L'_{lds} , L'_{lr} and L_{mq} are inductances of main winding, short circuit coil, rotor winding and mutual inductance between stator and rotor circuits. In (20) parameters of short circuit coil and rotor winding are referred to main stator winding.

In order simulation model to be complete it is necessary to add the equation for electromagnetic torque:

$$M_{em} = J \left(\frac{2}{P} \right) \frac{d\omega_r}{dt} + M_s \quad (21)$$

where: J is constant of inertia, M_s is load torque, P is number of pair of poles.

On the other hand electromagnetic torque can be found from:

$$M_{em} = \frac{P}{2} L_{mq} (i_{dr}^s i_{qs} - i_{qr}^s i_{ds}) \quad (22)$$

From (21) and (22) can be derived:

$$\frac{d\omega_r}{dt} = \frac{P^2 L_{mq}}{4J} (i_{dr}^s i_{qs} - i_{qr}^s i_{ds}) - \frac{P}{2J} M_s \quad (23)$$

Equations (20) and (23) are used to simulate transient performance characteristics of the shaded-pole motor.

In figures 7, 8, 9, 10 and 11 are presented transient performance characteristics during free acceleration, as follows: $n_r = f(t)$, $M_{em} = f(t)$, $I_1 = f(t)$, $I_3 = f(t)$ and $I_2 = f(t)$.

In order to carry out a deepened analysis of the shaded-pole motor, the transient performance characteristics are simulated at load torque, as well. As the motor is assigned for fan driving, having the static torque characteristic $M_s = k \cdot n^2$, the start-up transient characteristics at rated load are presented in figures 12, 13, 14, 15 and 16.

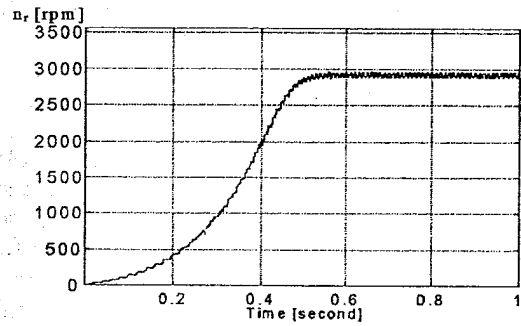


Fig. 7. Characteristic of speed at free acceleration

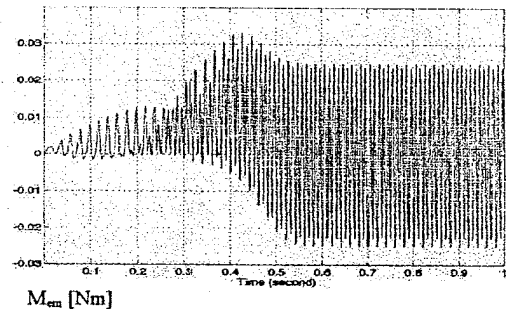


Fig. 8. Characteristics of torque at free acceleration

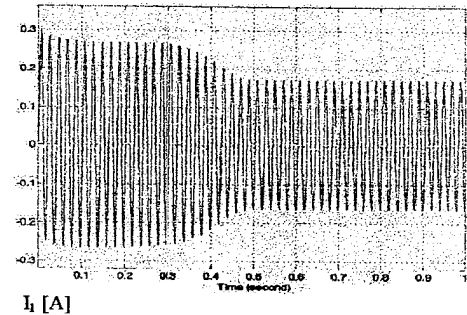


Fig. 9. Characteristic of main-winding current at free acceleration

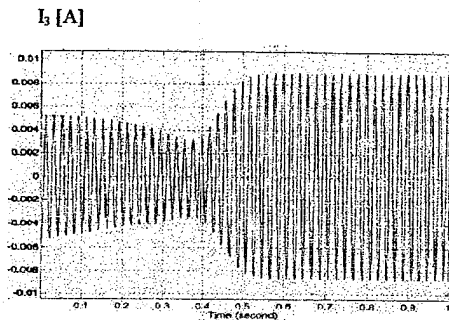


Fig. 10. Characteristic of short-circuit coil current at free acceleration

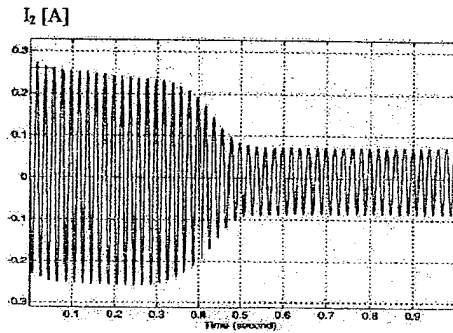


Fig. 11. Characteristic of rotor current at free acceleration

After the transients are suppressed, the motor reaches to the steady state regime. For the purposes of verification of the simulation model results for speed, electromagnetic torque and currents in all windings, are compared with results from CTM. The comparison, for free acceleration as well as for rated load condition, i.e. $s=0.16$, is presented in Tables II and III, respectively.

Table II
Comparative results MSM and CTM at free acceleration

	MSM	CTM
n [rpm]	2892	2910
M_{em} [Nm]	0.00167	0.0017808
I_1 [A]	0.12214	0.113365
I_3 [A]	0.00635	0.007692
I_2 [A]	0.049	0.0538

Table III
Comparative results from CTM and MSM at rated load

	MSM	CTM
n [rpm]	2250	2520
M_{em} [Nm]	0.00189	0.0018075
I_1 [A]	0.142	0.126
I_3 [A]	0.00338	0.0044
I_2 [A]	0.09638	0.087812

In addition, the motor model will be used for an analysis of the effect of parameters variation, on the starting characteristics of the motor. As an example in Fig. 17 and 18, the characteristic $n=f(t)$, for different shading portions of the stator poles, and for different rotor cage resistances are presented, respectively.

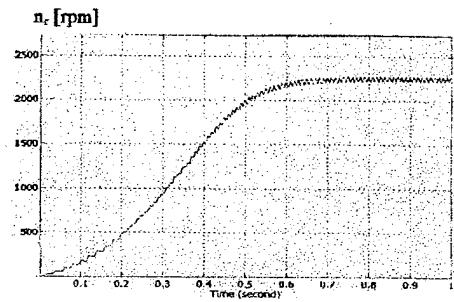


Fig. 12. Characteristic of speed at rated load

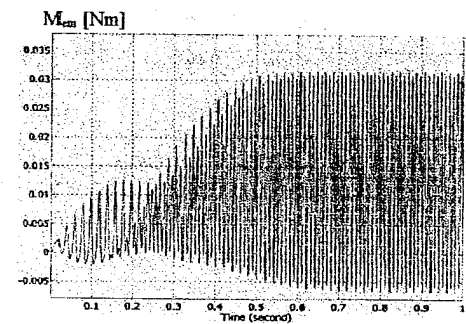


Fig. 13. Characteristic of torque at rated load

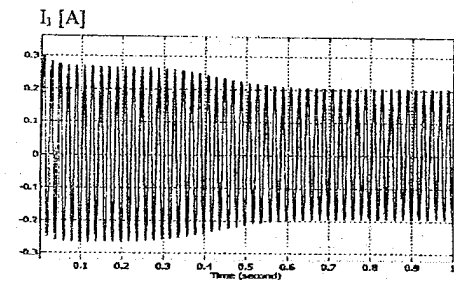


Fig. 14. Characteristic of main-winding current at rated load

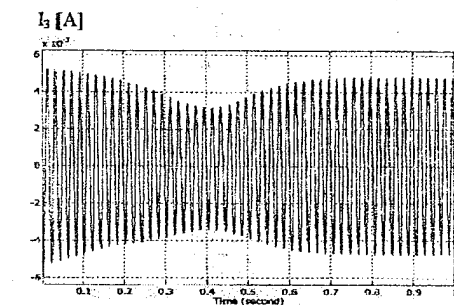


Fig. 15. Characteristic of short-circuit coil current at rated load

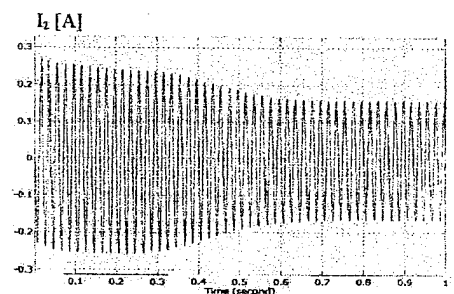


Fig. 16. Characteristic of rotor current at rated load

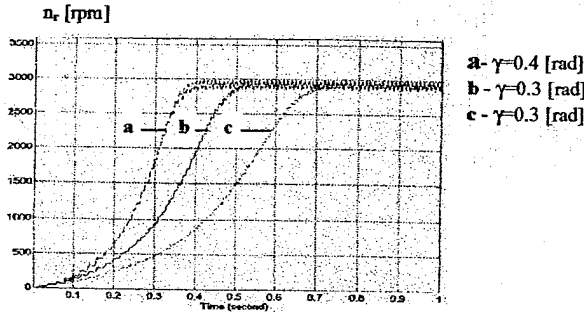


Fig. 17. Speed response at different shading portions

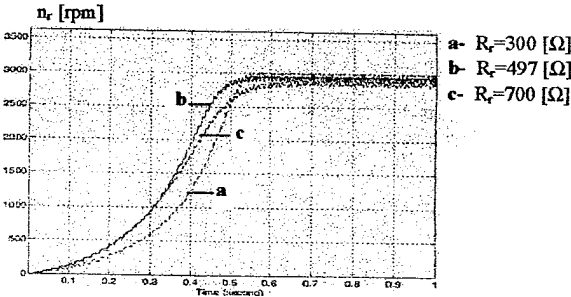


Fig. 18. Speed response at different rotor resistances

IV COMPARATIVE ANALYSIS

The proposed methodology based on different methods for calculation of characteristics under different operating conditions, enables the complex performance analysis of shaded-pole induction motor, to be carried out. The good way for evaluation of characteristics, obtained from steady state and transient analyses by using different methods, is to present a comparison of the results. Comparative static characteristics from CTM, FEM and MSM are presented in Fig. 19. Some of the most interesting values are extracted and given in Table IV. Additionally in Table V is presented comparison of motor characteristics obtained from CTM, FEM, MSM and the testing data at rated slip, $s=0.16$.

Table IV
Torque results by different methods

s [/]	Electromagnetic torque M_{em} [Nm]		
	CTM	FEM	MSM
0.01	0.001625	0.0017808	0.00167
0.10	0.012647	0.0156608	0.01141
0.16	0.018075	0.0199774	0.01890
0.30	0.022175	0.0196288	0.02023
0.50	0.018423	0.0147680	0.01639
0.80	0.008042	0.0088368	0.00800
0.99	0.001809	0.0028912	0.00200

Table V
Results by different methods, at rated slip

	CTM	FEM	MSM	Experiment
M_{em} [Nm]	0.018075	0.01997	0.0189	0.021
n [rpm]	2520	/	2250	2120
I_1 [A]	0.1259	/	0.142	0.125
I_3 [A]	0.0044	/	0.00338	/
I_2 [A]	0.087812	/	0.09638	/
cosφ	0.653888	/	/	0.654
P_{Fe} [W]	4.84	5.891	/	6.24

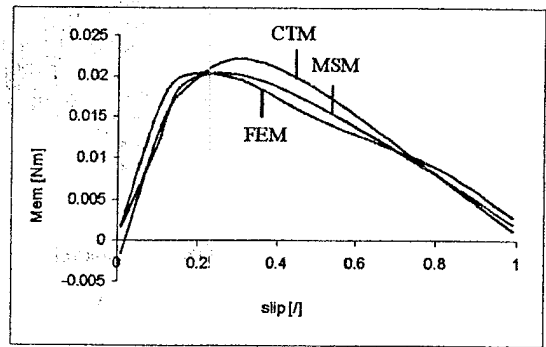


Fig. 19. Comparative torque slip characteristics by different methods

V. CONCLUSION

The paper is presenting an approach to the evaluation of steady state and transient performance characteristics of a shaded-pole motor. The authors start from the generalized theory of single-phase induction motor with asymmetrical windings and develop an analytical model based on the equivalent circuits. Special attention is put on exact determination of motor parameters, i.e. inductances, knowing that, up to now there is no generalized methodology. As a result motor electromechanical characteristics are determined.

The FE numerical method is used for calculation of static torque characteristics, too. By using the powerful simulation tool offered by Matlab/Simulink, the transient characteristics are determined at different operating modes. Results from all three methods applied are compared with data known from experiment, showing excellent agreement. On that way complex analysis of this special type of micro motor is performed, searching for as much as possible accurate methodology for determination of motor performance characteristics.

The next task is to include more parameters in calculations and to extend the analysis. This work could serve as a good guide.

REFERENCES

- [1] V. Sarac, L. Petkovska, M. Cundev, "An Improved Performance Analysis of a Shaded-pole Motor", *Proceedings of PCIM '01 Conference*, Vol. 2/3 p.p. 399-404, Nuremberg, Germany 2001.
- [2] I. E. Davidson, "Performance Calculation for a Shaded-Pole Single-Sided Linear Induction Motor Using Symmetrical Components and Finite Element Method", *Journal 'ELECTROMOTION'*, Vol. 4, No. 4, 1997, p.p. 139-145, Cluj-Napoca, Romania.
- [3] L. Petkovska, M. Cundev, V. Sarac, "FEM Analysis of Asymmetrical Magnetic Field in Electrical Machines", *Proceedings of ACOMEN '02 Conference*, on CD p.p. 1-10, Liege, Belgium, 2002.
- [4] A. M. Osheiba, K. A. Ahmed, M. A. Rahman, "Performance Prediction of Shaded-pole Induction Motors", *IEEE Transactions on Industry Application*, Vol. 27, No. 5, 1991, p.p. 876-882.
- [5] P.C. Krause, O. Wasynczuk, S.D. Sudhoff, "Analysis of Electric Machinery" IEEE Press, New York, 1995.
- [6] C. M. Ong, "Dynamic simulation of electric Machinery (using MATLAB/Simulink)", Prentice Hall PTR, New Jersey, 1998.

— Author Index to ELECTROMOTION, Vol. 10 (2003) —

- Abdollahi, S.E. 126, 397
 Abida, L. 538
 Aguglia, D. 180
 Ait-Amirat, Y. 365
 Akpinar, E. 211
 Alcaso, A.N. 673
 Amara, Y. 311
 Arshad, W.M. 400
- Bachir, S. 679
 Bak-Jensen, Birgitte 647
 Barazane, L. 27
 Belahcen, A. 381
 Belhadj, J. 449, 653, 663
 Ben Ahmed, H. 286, 311
 Benbouzid, M.E.H. 45
 Bendjebbar, M. 477
 Benreheb, M. 385
 Bensaker, B. 483
 Berkouk, E.M. 246
 Bertoluzzo, M. 217
 Betin, F. 455, 545
 Binder, A. 325
 Bitoleanu, A. 523
 Bizkevelci, E. 120
 Blissenbach, R. 420
 Boccaletti, Chiara 223
 Boglietti, A. 138, 506
 Boldea, I. 647
 Boltasu, D. 296
 Bouallaga, K. 292
 Bouchafaa, F. 246
 Boucherit, M.S. 27, 246, 489
 Bouhoune, K. 500
 Bounouara, M. 653
 Bououlid, B. 494
 Boyé, H. 444
 Bratitsis, M. 623
 Brochet, P. 359, 385
 Bruzzese, C. 223, 512
 Buja, G. 217
 Buyse, H. 229
- Cabral, C.M. 77
 Cai, Jumei 153
 Campeanu, A. 187
 Campian, H. 472
 Cancelliere, P. 461
 Canders, W.-R. 159
 Capolino, G.-A. 437, 455, 545, 702
 Caricchi, F. 330
 Casadei, D. 267
 Cavagnino, A. 138, 506
 Cazacu, D. 301
 Cecconi, V. 317
 Cengiz, C. 211
 Champenois, G. 301, 574, 679
 Chen, L. 165
 Cimuca, G. 410, 641
 Ciolan, Gh. 263
 Cirrincione, G. 437
 Cirrincione, M. 317, 437
 Ciumbulea, Gloria 659
 Colteu, A. 668
 Constantinescu, C. 171
 Couto, C.A. 77
 Craciunescu, A. 659
 Crescimbinì, F. 330
 Crivii, M. 132
 Cvetkovski, G. 353
- Dakyo, B. 635
 Darie, S. 416
 Da Silveira, M.A. 275
 De Donato, G. 330
 De Fornel, B. 449
 Delli Colli, V. 461
 Delmas, L. 551
 Dems, Maria 19
 Denes, I. 59, 556
 Dente, J.A. 579
 Derks, D. 359
 Diallo, D. 45
 Diop, D. 365
 Di Stefano, R. 461

- Djerdir, A. 371
 Dobra, P. 584, 590
 Dobriceanu, M. 523
 Draganescu, O.Gh. 193
- Ehsani, M. 126
 El Aimani, Salma 629
 El Amraoui, Lilia 385
 El Hajjaji, A. 391
 El Hassani, A. 377
 El Kadri, Khadija 371
 El Mokadem, M. 635
 Enache, S. 187
 Erdogan, N. 175, 568
 Ertan, H.B. 120
 Espanet, C. 240
- Faqir, A. 455
 Faucher, J. 93
 Feliachi, M. 12
 Ferraris, L. 138, 506
 Flores Filho, A.F. 275, 406
 François, B. 629
- Gabsi, M. 311
 Gair, S. 353
 Gameiro, Natalia S. 562
 Garcia, J.M. 659
 Garip, M. 568
 Gateau, G. 551
 Gay, S. 126
 Georgescu, M. 263
 Gergöz, O. 211
 Ghadiani, J. 397
 Ghita, A. 296
 Gillet, G. 668
 Gillon, F. 359, 385
 Giullii Capponi, F. 330
 Glises, R. 348
 Goncalves, Anabela 3
 Goyet, R. 292
 Grenier, D. 229
 Grisel, R. 175
 Guedda, M. 103, 477
 Gusia, S. 229
- Hackmann, W. 325
 Hanamoto, T. 691
 Harel, F. 348
 Hasni, T. 708
 Henao, H. 702
- Henneberger, G. 153, 420
 Hissel, D. 348
 Hoang, E. 286, 311
 Honorati, O. 330
 Hoshino, T. 144
 Hosseini, M. 397
 Hou, L.J. 165
 Husain, I. 574
- Ibtiouen, R. 500
 Ilea, D. 69
 Ionescu, A. 187
- Janulyte, Aurika 594
 Jufer, M. 132, 432
 Jung, H.J. 144
- Kamwa, I. 180
 Kang, D.H. 410
 Kasapoglu, A. 568
 Kasmieh, T. 93
 Kauffmann, J.-M. 348, 365
 Khasimov, A.A. 85
 Kherfane, H. 483
 Khojet El Khil, S. 685
 Koczara, W. 635
 Komez, K. 19
 Koo, D.H. 410
- Labrique, F. 229
 La Cascia, D. 317
 Lafore, Dominique 594
 Larabi, A. 489
 Larbes, C. 27
 Launay, A. 301
 Laza, F. 574
 Lazzari, M. 138, 506
 Leclercq, L. 641
 Lecrivain, M. 286, 311
 Libert, Florence 252
 Livadaru, L. 199
 Livint, Gh. 518
 Lobato, P. 579
 Luparia, G. 138, 506
 Lupsa-Tataru, L. 69
- Mailfert, A. 668
 Makouf, A. 45
 Marginean, C. 619
 Marignetti, F. 461
 Marques Cardoso, A.J. 562, 673

- Martis, Claudia 702
 Masson, J.P. 306
 Medromi, H. 377
 Metatla, M. 483
 Meynard, T.A. 551
 Michael, C. 336
 Micu, E. 606
 Mihai, D. 171, 533
 Mihet-Popa, L. 647
 Mininger, X. 280
 Minne, F. 629
 Miraoui, A. 116, 240, 258, 371, 416
 Mirsalim, M. 126, 397
 Mirzayee, M. 126
 Mitronikas, E.D. 467
 Moga, D. 584, 590
 Morar, A. 600
 Morel, L. 306
 Moreno, F.M. 659
 Morita, G. 144
 Mosebach, H. 159
 Mrabet, Olfa 663
 Munteanu, M. 584, 590
 Munteanu, R. 258, 416
 Munteanu jr., R. 584, 590
 Muta, I. 144
 Mutoh, N. 342

 Naceri, F. 538
 Naciri, M. 494
 Nagy, I. 59, 556
 Nahid-Mobarakeh, B. 545
 Nait-Said, M.-S. 12
 Nait-Said, N. 12
 Nakamura, T. 144
 N'diaye, A. 258
 Neamt, D. 606
 Neves, V. 3
 Nichita, C. 635

 Oguro, R. 691
 Ouiguini, R. 27
 Ozoglu, Y. 568

 Pages, O. 391
 Paicu, G. 518
 Pana, T. 472
 Pera, Marie-Cecile 348
 Peter, D.C. 606
 Petkovska, Lidija 205, 353
 Pietrzak-David, Maria 449

 Pina, Murta 3
 Pinchon, D. 455, 545
 Pires, A.J. 579
 Poloujadoff, M. 292
 Popan, A.D. 420

 Popescu, Mihaela 523
 Pucci, M. 317, 437

 Rabulea, O. 619
 Rachidi, M. 494
 Radulescu, M.M. 117, 574, 641
 Rinaldi, V. 406
 Ritchie, E. 647
 Roboam, X. 93, 653, 663
 Robyns, B. 629, 641
 Rodrigues, A.L. 3, 148
 Rossi, C. 267
 Rusu, C. 610

 Saadi, J. 377
 Safacas, A.N. 336, 527, 623
 Santini, E. 223, 512
 Sarac, Vasilija 205
 Saudemont, C. 641
 Schmidt, I. 234
 Sekiguchi, K. 342
 Sellami, Y. 27
 Serra, G. 267
 Sfetsos, A. 3
 Sido, Nana-Mariama 668
 Simion, A. 199
 Sixdenier, F. 306
 Slama-Belkhodja, Ilhem 449, 685
 Solero, L. 330
 Sordi, P. 223
 Soulard, Juliette 252, 400
 Stampacchia, E. 217
 Stoia, D. 263
 Suriano, G. 400
 Susin, A.A. 275

 Takita, K. 342
 Tani, A. 267
 Tekin, M. 348
 Teixeira, M.M. 659
 Tirnovan, R. 258, 416
 Tnani, S. 679
 Torac, Ileana 614
 Trifa, V. 619
 Tsimplostefanakis, E. 623

Tsoumas, I. 527, 623
Tsuji, T. 691

Umeda, N. 691

Vadan, I. 410
Veszpremi, K. 234
Vido, L. 311
Viorel, I.A. 420
Vlad, I. 187

Wamkeue, R. 180, 483

Xie, J. 697

Yalçiner, L.B. 120
Yazid, K. 500

Zago, S. 217
Zerikat, M. 103, 477
Zinger, D.S. 27
Zire, H.S. 240
Zito, P. 317
Zouaghi, T. 708
Zynovchenko, A. 697

ELECTROMOTION

Volume 10, Number 3
July - September 2003

ELECTROMOTION
MEDIAMIRA SCIENCE PUBLISHER
P.O. Box 117,
RO-400110 Cluj-Napoca 1, Romania

ISSN 1223 - 057X

